Air-coupled Ultrasound – Emerging NDT Method

Institut für Kunststofftechnik, Universität Stuttgart:
Wolfgang Essig, Yannick Bernhardt, Daniel Döring, Igor Solodov; *contact: wolfgang.essig@ikt.uni-stuttgart.de*
Sonotec GmbH: **Tobias Gautzsch;** *contact: Tobias.Gautzsch@sonotec.de*
Federal Institute for Materials Research and Testing: **Mate Gaal, Daniel Hufschläger;** *contact: mate.gaal@bam.de*
XARION Laser Acoustics GmbH: **Ryan Sommerhuber, Matthias Brauns;** *contact: r.sommerhuber@xarion.com*
Fagus-GreCon Greten GmbH & Co. KG: **Torben Marhenke, Jörg Hasener;** *contact: torben.marhenke@gmail.com*
Hillger NDT GmbH: **Artur Szewieczek, Wolfgang Hillger;** *contact: artur.szewieczek@hillger-ndt.de*

Introduction. Development of air-coupled ultrasonic testing

(Corresponding Author: Wolfgang Essig and Daniel Döring, Marc Kreutzbruck, Institut für Kunststofftechnik, University of Stuttgart, Stuttgart, Germany)

The historical development of air-coupled ultrasonic testing is difficult to follow, since it made massive use of developments in other acoustic disciplines. Thus, the driving force for the development of capacitive air-coupled ultrasonic transducers with matched impedance (1) was not material testing, but data transmission and distance measurement. Until today, manufacturers of such transducers mostly use piezo discs and matching layers of transducers for ultrasonic distance measurement (2). In 1971, special applications relied on the low speed of sound in air for plate wave excitation in thin materials such as paper (3), but with large capacitive transducers and thus hardly suitable for a reasonably spatially resolved measurement. The extreme impedance jump between air and practically all solid media was also seen as an advantage in air-coupled ultrasonic microscopy for surface topography, since the degree of reflection hardly depends on the material present and no additional signals from the interior of the test material are to be expected (4). Only advances in the design of air-coupled ultrasonic transducers from the 1980s onwards, which continue to this day (5–11), led to the development of a series of air-coupled ultrasonic testing systems, which also set themselves the goal of competing with conventional ultrasound in their niches. With the availability of these systems, research in NDT with air-coupled ultrasound expanded considerably. Subsequently, however, research concentrated on the use of air-coupled ultrasound with a focus on its suitability for industrial quality assurance, since the absence of a coupling agent is ultimately also a factor in cost reduction (12–14)

In principle, ultrasonic testing with air coupling has great potential to become a method for serial testing. Its economic advantages lie less in the relatively low procurement costs than in the uncomplicated integration into production processes. Apart from access to the component surface, air-coupled ultrasonic testing does not require any further prerequisites except for a distance of a few centimeters: No immersion tank with subsequent cleaning and drying of the components (ultrasonic immersion technology) or radiation protection shielding (X-ray, CT). Since no coupling medium is required, this method is also suitable for testing swelling and (water-) absorbing components. In addition, the influencing factor of the contact pressure is eliminated, so that there are no amplitude fluctuations or damage to the surface of the component.

Air-coupled ultrasonic testing is independent of the optical surface properties. Other non-contact NDT methods (speckle inferometry, thermography) quickly reach their limits in the case of shiny, too light or too dark surfaces, bare metal or transparency and require pretreatments with the mandatory subsequent cleaning of the surfaces. Even possible electrical conductivity of materials, which is a prerequisite for eddy current based methods, is not important for air-coupled ultrasonic testing.

In addition, the coupling of air-coupled ultrasound to guided modes (plate and surface waves) in the material enables a considerable expansion of the field of application. On the one hand, the spectrum of testable component geometries is extended, since, among other things, testing with one-sided accessibility is also possible. On the other hand, in addition to the imaging of material inhomogeneities (defects), a quantitative investigation of the elastic properties can be carried out via velocity measurements. This includes possible material anisotropies, which play a decisive role in modern fiber composites. Elastic waves not only respond to the properties of their carrier medium, but are also influenced by their immediate environment. They can therefore be used as sensors for process monitoring.

Recent Developments in Research and Application in the Field of Air-coupled Ultrasonic Testing

Testing systems for air-coupled ultrasonic testing differ from normal ultrasonic testing systems by the very high transmission voltages of often up to 800 V combined with square wave pulser optimized for low frequencies. Only with these special transmitters, it is possible to perform the burst excitation in the usual frequency range from 30 to 700 kHz with sufficient energy. Due to the combination of preamplifier and power amplifier in the receivers, test systems for air-coupled ultrasonic testing also have an extremely low inherent noise. Values in the range of < 1 nV / √Hz enable the high amplifier dynamics of up to 120 dB analog amplification, which is necessary to obtain a very good signal-to-noise ratio (SNR) even with highly attenuating materials.

Measurement Set Up

(Corresponding Author: Tobias Gautzsch, Sonotec GmbH, Halle (Saale), Germany)

For different applications different methods have been developed. Depending on accessibility transmission, re-emission or pulse-echo method can be used.

Transmission Method

Air-coupled ultrasonic testing in transmission (see Figure 1) is the most common measuring method to detect the common defects in modern multilayer composites. These include delaminations, air inclusions, kissing bonds and impact damage. Each of these types of flaws leads to the formation of two additional boundary layers, which must be overcome by ultrasound. At each boundary layer, a transmission or reflection loss occurs (e.g. for a thick CFRP plate

of approx. 40 dB). The exact value can be calculated based on the sound velocity and density of the test medium. As soon as an additional flaw generates further interfaces at the sound path in the material, the amplitude loss is doubled.

Despite the use of air as coupling agent, small defects can be detected with air-coupled ultrasound. With a wavelength of 0.85 mm in air at 400 KHz ultrasound, defects as small as approx. 1 mm can be detected with a correspondingly small scanning grid. The transmission measurement is usually performed perpendicular to the component. For certain types of components or defect geometries, an oblique transmission can provide even better results. (15)

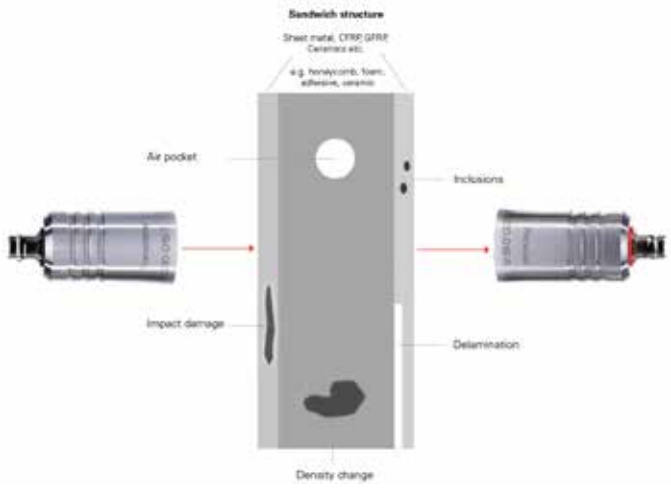

Figure 1: ACUT with transmission method of a sandwich structure and detectable defect scenario

Pulse-Echo Method

The major disadvantage of air-coupled ultrasonic testing in transmission is that it requires access to the test component from both sides. This can be remedied by testing in pulse-echo or by testing with guided waves.

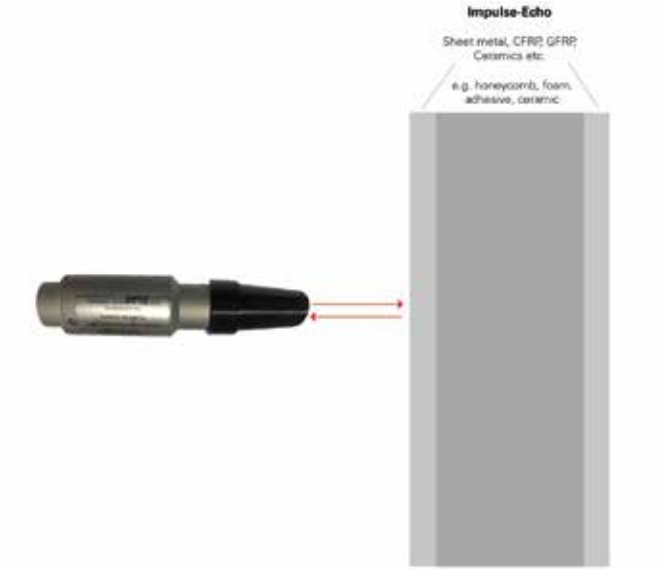

Figure 2: ACUT with the Impulse-Echo Method

The simplest one-sided measurement method is the pulse-echo measurement (see Figure 2). This method is the most commonly used method in classical water-coupled ultrasonic testing. In air-coupled ultrasonic testing, the pulse-echo principle is mostly used in distance measurement, for example in modern parking aids. In component testing, it is only of limited use due to the long wavelengths, long pulse durations and the large amount of reflection. The back-wall echo from the component is approx. 80 dB quieter than the surface echo (if the material has the same specific acoustic impedance as epoxy resin) and can usually not be separated from the surface reflection. A similar method is pitch catch, where a separate transmitter and receiver are applied using a similar setup as for pulse-echo. Up to now, pitch-catch method has been successfully used for testing concrete components (16) and woods (17) . Due to the very short wavelengths of sound in air, the pulse-echo method is also suitable for the precise inspection of component surfaces.

Re-Emission Method

A one-sided measuring principle more frequently used in air-coupled ultrasonic testing is the measurement with guided waves. In this measuring arrangement, shown in Figure 3, a guided wave is generated in the component by a specific inclination of the air-coupled ultrasonic probe. Specific types of guided waves are defined based on their pattern of wave propagation. Plate waves travel in components with a thickness below a few wavelengths. In particular, plate waves in a homogeneous isotropic material are called Lamb waves. Rayleigh waves propagate at the component surface in components with thicknesses significantly larger than the wavelength. The transition between plate waves and Rayleigh waves is smooth. This test method makes use of the fact that the plate wave velocity depends on the frequency and thickness of the component and can be excited and detected by narrow-band air-coupled ultrasound. Defects in the component lead to reflections or speed changes of the wave. These effects can be detected and evaluated by measuring the ultrasound emitted from the surface. However, the advantage of the one-sided test is at the expense of a distortion of the test result by the travel distance of the plate wave in the test object. This must be chosen long enough for the measurement signal to stand out from the surface reflection. Alternatively, a sound shield can be used between the probes, but this does not make the procedure completely contactless. (15, 18, 19).

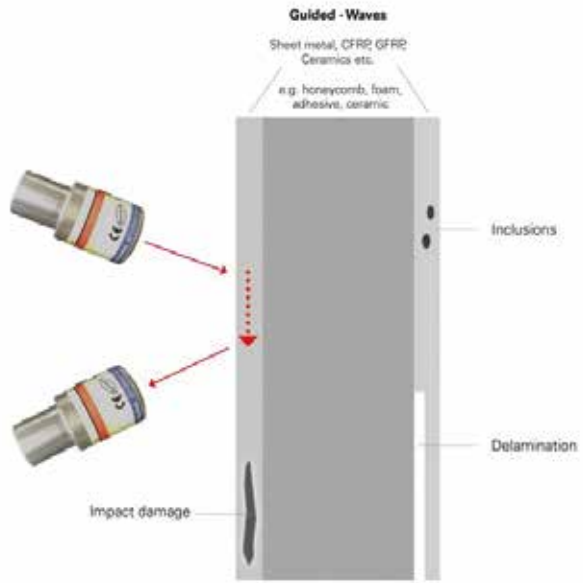

Figure 3: ACUT in re-emission method using guided waves and detectable defect scenario.

Full-field excitation and full-field imaging

(Corresponding Author: Yannick Bernhardt, Igor Solodov and Marc Kreutzbruck, Institut für Kunststofftechnik, University of Stuttgart, Stuttgart, Germany)

A widely-used NDT inspection method is based on monitoring transient elastic excitations in solids (acoustic emission (AE)) that occur when a material undergoes irreversible changes in its internal structure (20). The waves are generated by momentary release of strain energy due to material micro-cracking and are traditionally detected by using ultrasonic transducers attached to the test surface. To determine the damage location the transducers are arranged in arrays to apply beamforming computation tool (21–23) .

Recent studies show that conventional (internal) acoustic emission can also be accompanied by “external” AE events and, therefore, detected remotely e.g. by air-coupled transducers (24). An alternative approach for detecting and locating of sound sources in air is concerned with the use of the beamforming method in acoustic microphone arrays (acoustic cameras) (25). The algorithm represents the region of interest as a grid of virtual sound sources whose signals are phase shifted due to various time delays. By drawing the root mean square of the signals over the area of interest an acoustic image is generated. Most applications of acoustic cameras are focused on monitoring noise outside and inside transportation vehicles (from cars to trains and airplanes).

For this reason, commercial acoustic cameras mainly operate in audible frequency range and cannot be directly applied for conventional ultrasonic imaging of defects where the frequencies of some hundred kHz are required for reasonable resolution (26).

The feasibility of this technique is demonstrated below using the acoustic camera SoundCam by CAE systems, Gütersloh, Germany, provided by Wölfel GmbH, Würzburg, Germany. It contains 64 MEMS-microphones, a data acquisition system with 24-bit resolution, sample rate 48 kHz with an operating frequency range between 10 and 24 kHz. The setup to provide full-field resonant air coupled emission (RACE) imaging is shown in Figure 4. The camera operation included the adjustment of the distance to the sound source, the dynamic range and the frequency of the receiver.

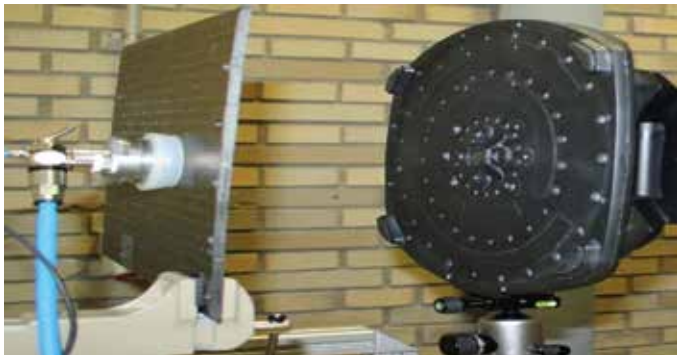

Figure 4: SoundCam setup for full field RACE imaging

To test the acoustic camera operation, the acoustic field of the piezo-actuator (isi-sys) was visualized first (Figure 5). As one can see from the picture, the active zone of acoustic field of the vacuum attached transducer (diameter 5 mm) is highlighted with a bright spot. This circular spot indicates the position where the sound amplitude is maximal, which matches to the real active zone of the transducer. The SoundCam interface also shown in Figure 5 indicates reasonably high (>10 dB) dynamic range of the image and a fundamental frequency radiated (~13100 Hz).

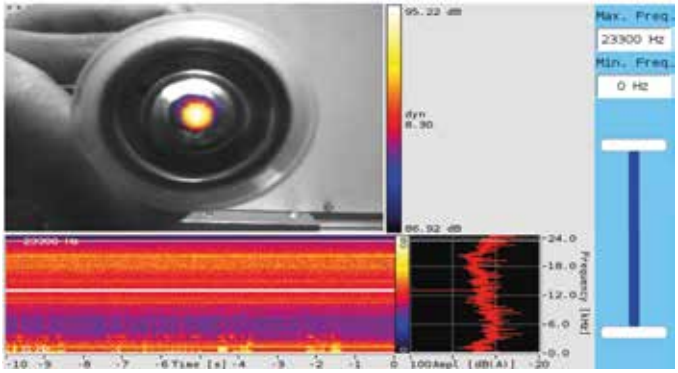

Figure 5: Interface of SoundCam and full-field image of acoustic field for isi-sys transducer (frequency 13100 Hz).

The vacuum attached transducer was then used in the noisy mode for the RACE excitation in a PMMA plate with two flat bottom holes (Figure 6). The laser vibrometry test reveals different local defect resonance (LDR) frequencies for those holes (Figure 6, a, b). The frequency bandwidth of the SoundCam receiver was then narrowed down around the value of the LDR frequency (12200 – 13300 Hz, Figure 6, d) to demonstrate consecutive frequency-selective RACE imaging of the defects.

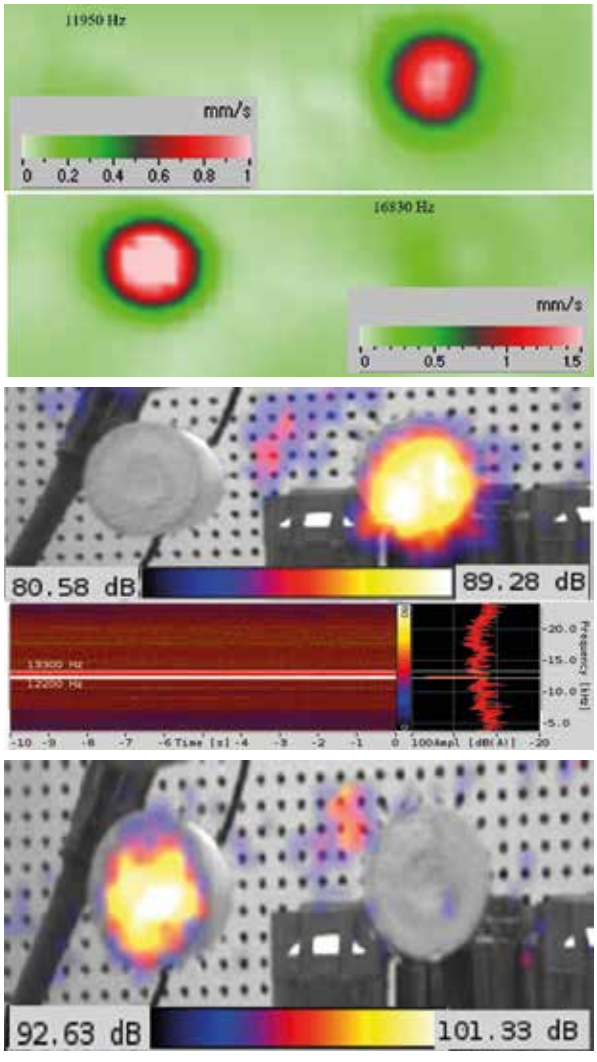

Figure 6: Frequency-selective full-field RACE imaging (c, d) and laser vibrometry (a, b) for a pair of circular FBH of different LDR frequencies.

Full-field scanning can be applied for imaging of not only simulated but also some realistic defects as demonstrated in Figure 7 a, b, for an elliptic delamination above the actuator imbedded in a Glass Fiber Reinforced Polymer (GFRP) plate. The active part of the delamination responds to LDR excitation at frequency 18900 Hz and is seen in the laser vibrometry scan (Figure 7, b). Full-field RACE excited at this frequency (Figure 7, a) clearly indicates the resonance part of the delamination but requires much less time for testing.

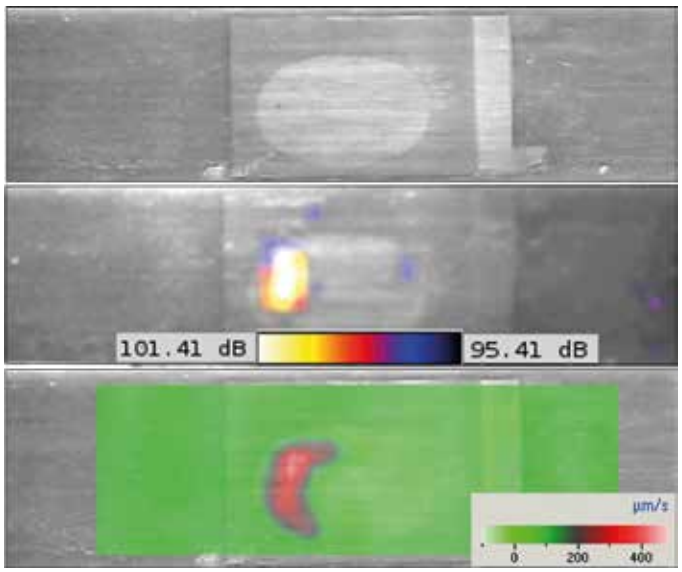

Figure 7: SoundCam imaging of a delamination in piezo-actuator imbedded in GFRP plate (a), 18900 Hz LDR laser vibrometry image of the delamination (b)

An application of RACE for full-field imaging of defects in a lap joint is shown in Figure 8, c, d. The joint is made by gluing the flanges of the rectangular steel profile (500 mm x 50 mm x 65 mm) to 1.5 mm steel base. The disbond (length~40 mm) is simulated by the lack of adhesive between the flange and the base (inside the white rectangular in Figure 8, c). A piezoelectric transducer is attached to the reverse side of the base and excited with 20 V noise signal. The two bright spots in Figure 8, d) disclose the acoustic waves generated by the transducer (left) and the RACE field radiated by the disbond area (right).

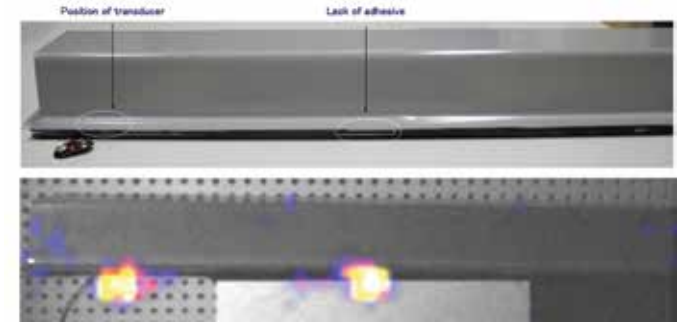

Figure 8: SoundCam imaging of a steel profile with adhesive disbond (c) and full-field RACE image of the disbonded area (d)

Research in Transducer Technology

Besides the commonly used transducers based on piezo discs with a matching layer or piezo composites several new ways of excitation are investigated.

Optical Microphone and Laser Excitation

(Corresponding Author: Ryan Sommerhuber and Matthias Brauns, XARION Laser Acoustics GmbH, Vienna, Austria)

A novel Laser-excited Acoustics (LEA) technology approach is introduced that solves many of the issues associated with the conventional techniques discussed above. In LEA, the setup is as follows: an excitation laser serves as the pulser and generates the ultrasound signal, while an optical microphone acts as the receiver (27, 28). LEA can operate in both standard arrangements for ultrasonic NDT: 1) through-transmission testing with excitation laser and optical microphone on opposite sides of the sample, and 2) single-sided testing, where both sender and receiver are on the same side of the sample in a pitch-catch configuration, as illustrated in Figure 9.

In contrast to most commercial systems available for conventional laser ultrasound, in LEA the visible or near-infrared excitation laser is fiber-coupled, which enables a very compact sensor head design for both single-sided pitch catch and through-transmission setups.

The pulse from the excitation laser is absorbed by the sample and generates a thermoacoustic shockwave directly below the surface. This broadband and impulse-like ultrasound shockwave propagates through the material, where it scatters off structural features. It then couples out from the sample into the air, where the optical microphone detects the airborne leaky wave.

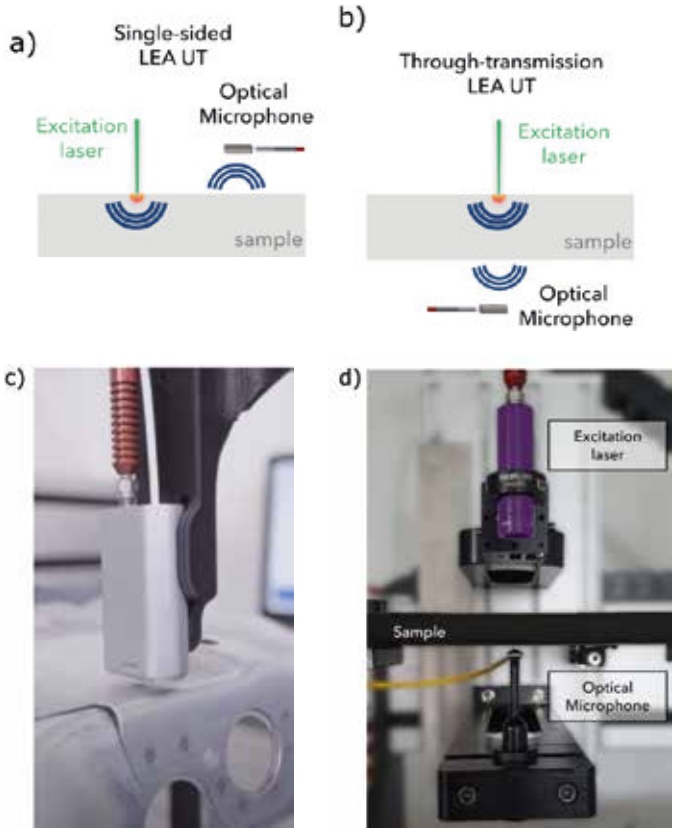

Figure 9: a) and c) Single-sided arrangement, and b) and d) through-transmission arrangement of excitation laser and optical microphone in LEA.

The detection principle of the optical microphone is based on laser interferometry. Inside the sensor head, there is a small air cavity formed by two semi-transparent mirrors. From a glass fiber, a laser beam couples through one of the mirrors into the cavity, which can host a multiple of the laser's wavelength, so that the laser light constructively interferes. The light partly couples back into the

glass fiber, where a photodetector converts it to a voltage signal. Sound and ultrasound alter the refractive index of the air, which affects the laser's wavelength in the cavity. The output voltage of the photodiode therefore linearly measures the sound pressure over a frequency range extending from 10 Hz all the way up to 2 MHz. Over this large bandwidth, the frequency response is flat due to the detection principle, which does not involve any mechanical movement. In many instances, this also reduces the effective blind zone associated with piezoelectric transducers.

Since the ultrasound waveform is measured directly in air, the ultrasound does not need to couple into a solid as it does for a piezoelectric receiver. This greatly enhances the SNR associated with the measurement setup. At the same time, the ultrasound detection process is not affected by the optical quality of the sample surface (e.g. roughness). Furthermore, both the excitation laser and the optical microphone are still operational even with an off-normal misalignment of ±5 degrees. These features, combined with the compactness of the all-fiber-coupled probe head (dimensions approx. 35 mm x 17 mm x 50 mm), make LEA a viable contact-free alternative for nondestructive testing for parts with complex geometry and composition.

To assess the capabilities of LEA, measurements were performed on a honeycomb core sandwich panel with a glass-fiber reinforced polymer (GFRP) skin (Figure 10a). The panel measured approximately 620 mm long by 230 mm wide by 13 mm thick and exhibited various reference defects (see the defect map in Figure 10a). The standard NDT method used in industry for such parts is water-coupled through-transmission ultrasonic testing operating at a frequency of 0.5–1 MHz.

a)

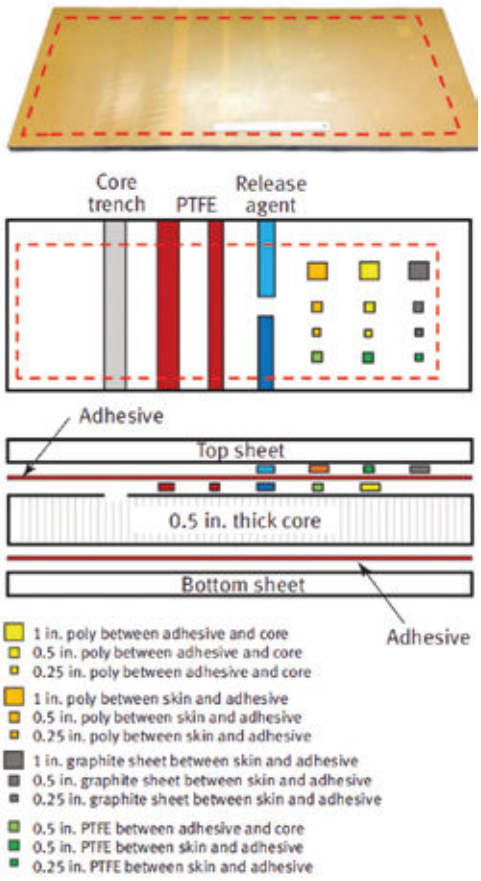

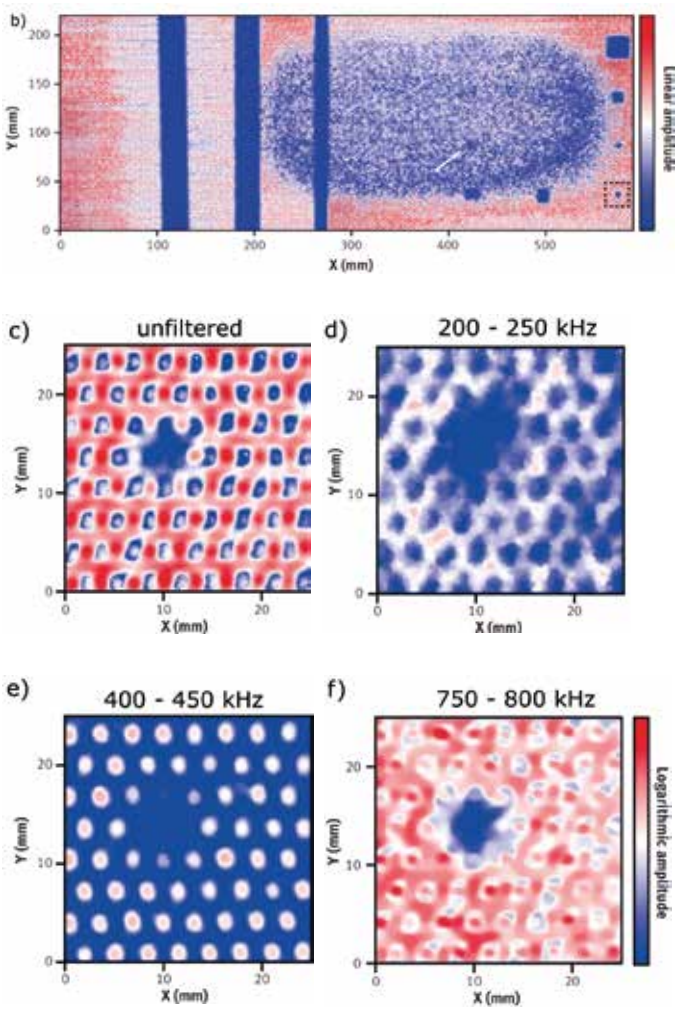

Figure 10: a) Specimen for demonstration of the LEA method. b) C-scan of the whole specimen. c–f) high-resolution C-scan of smallest defect with different frequency filters applied in post processing..

For the experimental setup, which is described in further detail in (29), the excitation laser and the optical microphone were mounted to the probe head of an automated X-Y scanning table. With the sample fixed in position, the probe head was scanned across the sample area indicated by the red dashed lines in Figure 10a. The step size was 0.5 mm in both X- and Y-direction, far below the size of any defined defect and smaller than the honeycomb pitch of 3 mm. This ensured the scan resolution was limited by the resolution of the LEA setup itself, not by the scanning step size. However, the scan step size can be deliberately chosen to other values such as 1 mm or 2 mm. Every pulse of the fiber-coupled excitation laser corresponded to one measurement point on the sample with no waveform signal averaging. Hence, the pulse repetition rate together with the step size, defined the scan speed. Different fiber-coupled excitation laser configurations have been tested with pulse repetition rates between 20 Hz and 10,000 Hz. Additionally an 8-channel array has been developed with a pitch of 2 mm, which boosts the inspection speed even further by a factor of eight.

The C-scan of the complete sample is shown in Figure 10b. While most reference defects were easily distinguishable, this was not true for the release agent and poly defects (blue, orange, and yellow in the defect map).

Their position correlated with the large oval region of decreased signal amplitude extending over the right half of the sample. Here, the top sheet was unintentionally unbonded from the honeycomb core due to the accidental spread of the release agent, which masked the underlying defects in the C-scan.

In order to demonstrate the measurement resolution of LEA, we zoomed in on one of the smallest defects present in the sample, a 6.35 × 6.35 mm PTFE insert between the top sheet and the adhesive film, as indicated by the dashed-line square in Figure 10b. Here, we performed a high-resolution scan with a step size of 0.2 mm, as shown in Figure 10c. In addition to the clearly visible defect, we also observed the honeycomb structure with high resolution.

Due to the large frequency range of the ultrasound waveform from 50 kHz up to 2 MHz, advanced frequency post-processing methods can be used, which are not possible with narrowband, air-coupled transducers. Here, we applied different bandpass filters to the data in Figure 10c as shown in the C-scans in Figure 10d–f. For frequencies between 200 and 250 kHz, the transmitted signal was dominated by guided wave modes propagating through the honeycomb cell walls (Figure 10d). The signal amplitude inverts for frequencies between 400 and 450 kHz, where the ultrasound passed almost exclusively through the air columns in the holes of the honeycomb structure (Figure 10e). In Figure 10f, a bandpass filter between 750 and 800 kHz was applied. In this frequency range, there was low contrast between honeycomb walls and the air columns, leading to a more uniform C-scan. The only region with a significantly lower signal amplitude was the PTFE reference defect, providing enhanced contrast between the defect and the honeycomb structure.

This example demonstrates that the post-processing of the LEA broadband data provides enhanced opportunities to selectively inspect the honeycomb walls, cell cavities, and any structural discontinuities. With conventional liquid-coupled or air-coupled ultrasound, this type of expanded analysis would not be possible without performing multiple measurements at different frequencies.

Ferroelectret Transducer

(Corresponding Author: Mate Gaal and Daniel Hufschläger, Federal Institute for Materials Research and Testing, Berlin, Germany)

Ferroelectrets are defined as charged cellular polymers exhibiting piezoelectric and pyroelectric properties (30-32). In some recent publications they are also referred to as piezoelectrets. Their strongly anisotropic cellular structure gives them extreme softness in one direction, which is also the direction of their polarization. Although they were named after ferroelectrics (or piezoelectric materials), the underlying mechanism of their piezoelectric properties is different and can be derived from the theory of capacitive microphones and loudspeakers. (33)

Typically ferroelectrets are about 100 µm thick films, which can be glued on an electrode, while the other electrode is deposited using electron beam evaporation at the other surface (34, 33). Spherical focusing combined with high-voltage excitation creates sound pressure levels above 140 dB (35). They can be excited using unipolar square pulses with 1.8 kV and their typical resonance frequency is between 200 and 300 kHz. Compared to some commercial transducers, they have a 20 dB higher signal-to-noise ratio. Ferroelectret transducers were applied to testing adhesive joints and fiber-reinforced plates, successfully detecting 1 mm sized inserts within joints and plates with a thickness about 4 mm. The sensitivity of a ferroelectret receiver can be increased by applying additional bias voltage, leading to an increase of the signal height by 12 to 15 dB. Some manipulation of the frequency is possible: transducers made of stacked layers exhibit lower resonance frequencies, but the price to pay is some decrease of sensitivity. (34, 36, 37).

Various transducer geometries can be easily created by structuring the backing electrode. This is how ferroelectret phased array probes were constructed (38). Another example of a structured electrode is a twin transducer consisting of a ring-formed and a circular electrode, where the transmitter and the receiver are parts of the same piece of ferroelectret film (39). The electrodes were placed on the same spherically focused circuit board, with curvature radius of 50 mm. As shown in Figure 11 (a), the inner electrode was a circle with a varied diameter and the outer electrode a ring around that circle with an outer diameter of 27 mm. The structure of the electrodes and the division into the transmitting and the receiving part are not visible on the photo in Figure 11 (b) because the outer electrode was evaporated over the whole surface of the twin transducer.

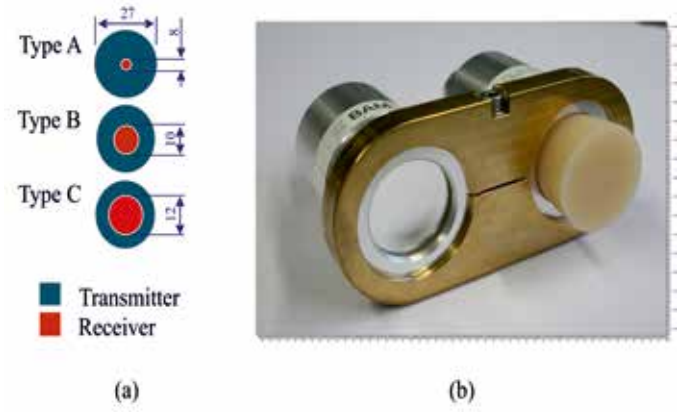

Figure 11. (a) The layout of the electrodes and (b) a photography of the ferroelectret twin probe. The electric units for the transmitter and for the receiver are placed in separate housings.

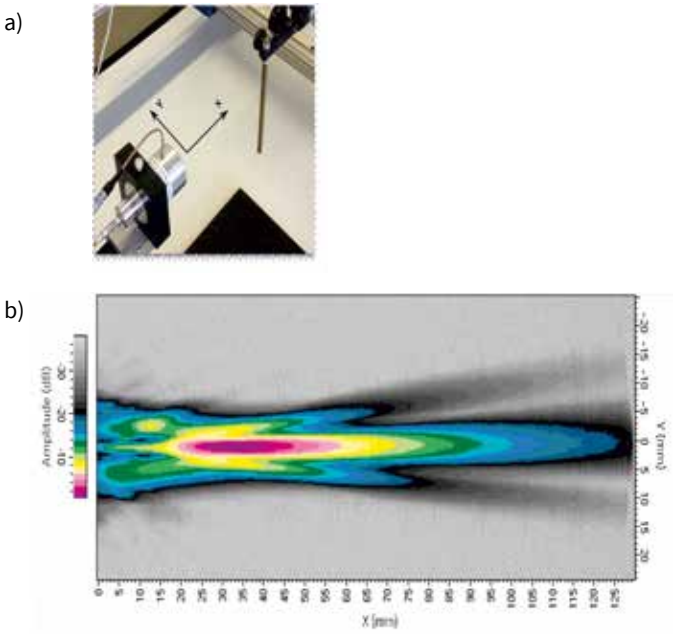

Figure 12. The sound field of the twin probe Type B recorded as a C-Scan of the reflection from a circular rod with a diameter 6 mm. The transducer was positioned at x = – 9 mm, y = 0 while the rod was moved. (a) The experimental setup and (b) the resulting C-Scan.

The sound field of this transducer was evaluated according to the norm ISO EN DIN 12668-2 describing immersion technique, with adjustments necessary to account for the medium air. The reflection from a circular rod (see Figure 12 (a)) with a 6 mm diameter was recorded and evaluated as a C-Scan (Figure 12(b)). The sound field resembles a sound field of a circular focusing transducer. The 6dB focal size depends on the relative size of the receiver, which is the circular electrode in the middle. For the receiver diameter of 8, 10 and 12 mm the focal sizes of 6.5, 3.1 and 3.7 were measured respectively.

Thermoacoustic Emitter

(Corresponding Author: Mate Gaal and Daniel Hufschläger, Federal Institute for Materials Research and Testing, Berlin, Germany)

We all know thunder and lightning, but rarely give a second thought to the physical mechanism behind the acoustic part of this phenomenon. The working principle is that the electrical discharge of the cloud rapidly increases the local temperature gradient, which generates the rumble of thunder. The pressure of the fluid propagates as shock wave front, travelling kilometers until it vanishes. The first scientific observations of thermoacoustical phenomena were reported by Byron Higgins who described the generation of sound during glass blowing process (40). Nowadays there are plasma speakers available on the market, which make use of thermoacoustic effect to reproduce audible sound.

Optimized for the ultrasonic range, there are thermoacoustic transducers consisting of a thin conductive layer based on fused silica. Electrical energy is converted to heat by Joule's heating, which is responsible for a sudden increase of the air pressure, initiating an acoustic wave. The first applications of such transmitters in non-destructive testing included a transmission of a 4 mm thick CFRP test piece (41), using a ferroelectret receiver.

Another possibility to use the thermoacoustic effect to produce ultrasonic waves is to use gas discharges (electric spark or arc), which brings us back to lightning and thunder. Acoustic measurements on electric spark discharges up to 500 kHz were performed (39). Electric spark is a form of plasma. It could be shown recently that the acoustic emission of plasma is shaped by two different effects. One of them is the thermoacoustic effect and the other one is an electrodynamic effect sometimes referred to as ionic wind, which relies on the production of charged particles and the body force caused by the electric field acting on these. Since the applied electrical field accelerates the charged particles, which interact with neutral particles, there is an increase in total energy. Elastic and inelastic collisions between charged (electrons, ions) particles and neutral molecules of the gas mixture cause the temperature increase.

A simple experimental setup was used to study the acoustic emission of gas discharges, as shown in Figure 13, with 1 mm distance between the electrodes and a pulse with 7,5 kV. Laser doppler vibrometer was applied to record the acoustic response as described in (41).

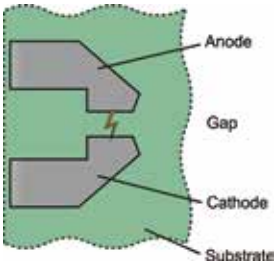

Figure 13. Schematic representation of the initiation of an electric spark.

The recorded signal (Figure 14) was very broadband, consisting of several distinguishable resonance frequencies with different amplitudes (39). Although the acoustic response strongly depends on the environmental settings, similar acoustical characteristics were reproduced over a period of one year without any modifications on the experimental setup. Several types of gas discharges were tested and an electric spark could produce a maximum sound pressure level of about 137 dB which is comparable to commercial transducers.

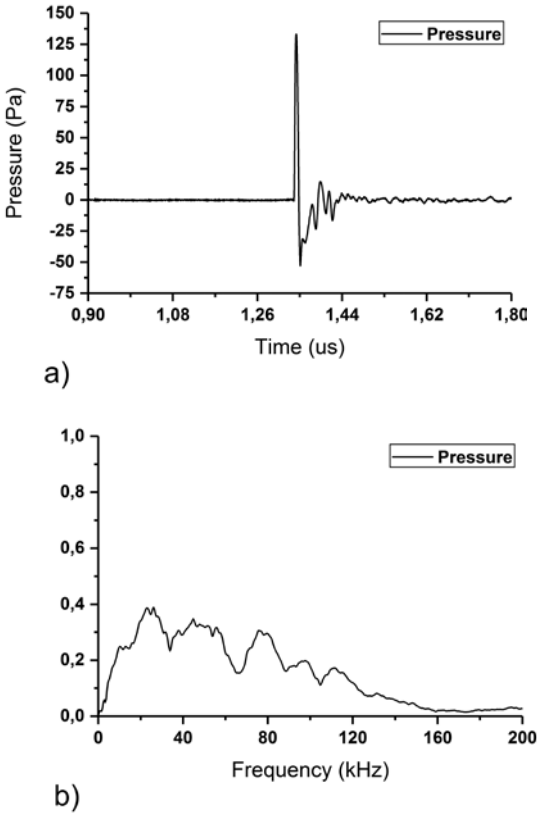

Figure 14. (a) Measured acoustic excitation of a gas discharge and (b) the corresponding Fourier transformed. The acoustic signal was recorded at 440 mm distance from the source.

Application in Industrial Environment

In the Article various methods are introduced that work quite well in research labs. However, ACUT is not only a research topic. There are many existing scenarios where ACUT has been and is used in industrial environment.

Automated Weld Testing

(Corresponding Author: Ryan Sommerhuber and Matthias Brauns, XARION Laser Acoustics GmbH, Vienna, Austria)

Spot welding has become a common technology for joining the parts of a car body. This process is highly automated, ensuring a high degree of process control at low cost, and making it compatible with high-volume production. The inspection of at least a subset of the spot welds on each car body is a core part of the production process due to the high demands of quality control in the automotive sector. In contrast to the spot welding process itself, the inspection of the weld spots is routinely performed manually by ultrasonic testing. This manual inspection is associated with high operating costs for dedicated inspection personnel working in

shifts. Furthermore, the results from manual inspection are inherently subjective and prone to human error, which clashes with the ever-increasing demand for objectivity, reproducibility, and complete documentation of inspection results (42, 43).

Therefore, car manufacturers have tried to automate ultrasonic testing methods for many years, but this remains challenging for two main reasons:

1. Sub-millimeter alignment accuracy of the sensor head with respect to the spot weld is needed, making 3-D measurements of the spot weld location necessary (e.g. with a camera) (42).
2. The sensor head needs to be either coupled to the weld by a liquid coupling agent, or the sensor head needs to be in physical contact with the weld surface itself, making it sensitive to surface properties like weld tool imprints or roughness (42, 43).

These obstacles can be overcome by contact-free approaches using acoustic Lamb waves (44, 45) instead of the backwall echo commonly used for evaluation in manual UT methods. To achieve a sufficient signal-to-noise ratio (SNR), contact-free excitation and detection of ultrasound can be done using an excitation laser and a laser-based optical microphone instead of piezo-elements. This approach is called Laser-excited Acoustics (LEA). It overcomes the double acoustic impedance barrier that limits the usability of air-coupled piezo-elements (46), and enables the single-sided, contact-free inspection of spot welds in steel sheets.

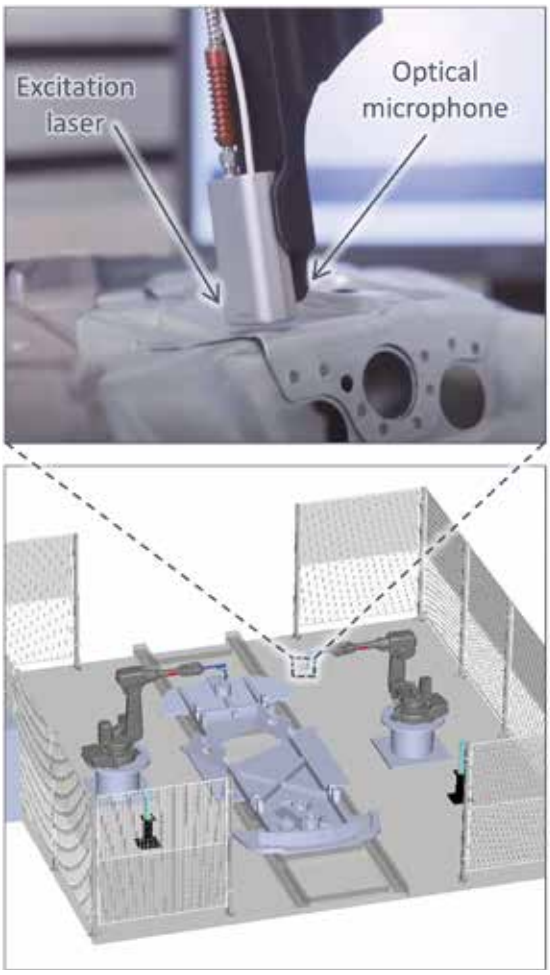

Figure 15: Fully automated LEA cell for spot-weld inspection with two industrial robots performing the testing. No physical contact between steel and sensor head is required.

In LEA, the excitation laser shoots a short laser pulse on the upper metal sheet for each measurement point, which locally heats up the surface on a nanosecond timescale, and causes a broadband impulse-like ultrasonic shockwave via the thermoacoustic effect. In thin solids like metal sheets, this excites a Lamb wave, a collective movement of the whole sheet, which propagates within the sheet plane (see Figure 18). Since the group velocity of the Lamb wave depends not only on the frequency , but also on the sheet thickness, it is scattered at the suddenly changing effective sheet thickness in the area of the spot weld, and partly undergoes a mode conversion (44). Effectively, this leads to a reduced amplitude of the ultrasound waveform after propagation through the spot weld. At the point of detection, the optical microphone detects the ultrasound waveform leaking into the air.

Since the optical microphone detects the ultrasound directly in air by means of laser interferometry (44, 27), it avoids the double acoustic-impedance barrier of air-coupled piezoelectric transducers, where a lot of signal is additionally lost at the interface between air and piezo material. Therefore, the sensitivity of the optical microphone is high enough to perform the inspection on spot welds in aluminum as well as steel sheets (44).

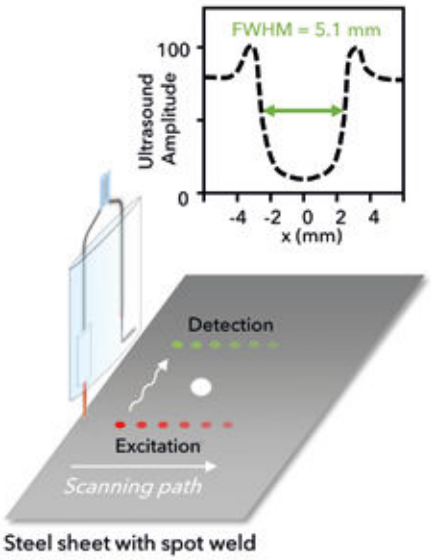

Figure 16: The measurement principle of LEA. The full width at half maximum (FWHM) of the profile corresponds to the inner weld nugget diameter.

The excitation laser and the optical microphone are combined into a single sensor head that performs the ultrasonic testing of the spot weld hovering several millimeters above the part surface (see Figure 17).

For the inspection, the robot uses the CAD data of the part under test to drive the sensor head to a fixed position above the spot weld. Subsequently, the sensor head scans along the spot weld, while shooting laser pulses at a repetition rate of several hundred Hertz. By evaluating the received waveform, an amplitude profile is generated (see Figure 18). Since the signal is attenuated at the positions where the Lamb wave propagates through the spot weld, the width of this dip in the profile corresponds to the weld nugget diameter. This approach is robust against alignment inaccuracies within the sheet plane, as long as the weld spot is located between excitation laser and optical microphone, and against inaccuracies in distance to the surface as long as the airborne signal still provi-

des a sufficient SNR, leading to a tolerance of several millimeters in all three dimensions. The complete scanning procedure takes approximately five seconds per spot weld.

Automated Wood Testing

(Corresponding Author: Torben Marhenke and Jörg Hasener, Fagus-GreCon Greten GmbH & Co. KG, Alfeld, Germany)

Since wood-based materials consist of several structural elements bonded together with glues and additives, there is a risk of air pockets or areas that are not or insufficiently glued (here called delaminations) which lead to reduced load-bearing capacities and increase the risk of structural failure. Such delaminations usually occur at the press exit, when the plates leave the press. The following reasons or causes lead to delaminations and can be divided into the following groups:

1. Excessive moisture content in the board, which is due to excessive moisture content of the wood particles or also glue that is too rich in water or a high degree of gluing. In the press, the boiling point of water is not reached due to the high pressure. On leaving the press, the pressure decreases abruptly and spontaneous vapor formation occurs. The resulting vapor pressure increases with the moisture content and can lead to delaminations.
2. Too short pressing times, which prevent sufficient curing of the glue. The weakly developed adhesive bonds between the individual structural elements result in a reduction of the binding forces of the glue and thus defects occur despite a correct moisture content.
3. Insufficient possibilities for the board to evaporate. Reasons are, for example, too high content of fine particles or irregular spreading, which prevents part of the resulting vapor pressure from escaping from the board.

Ultrasonic testing has become well established in industrial applications for the detection of splitting and press control. In particular, air-coupled ultrasound (ACU) is used because it does not require coupling media such as water or gels that lead to residues on the plate. ACU measurement is mainly performed in transmission (47). A transducer on one side of the plate emits ultrasonic pulses that are received on the other side of the plate. In the case of a delamination, an amplitude drop occurs at the receiver, through which the delaminations are detected (see Figure 1).

A disadvantage of the ACU method is that there is a large difference in acoustic impedance between wood-based materials and air. Consequently, strong reflections occur at the transition between the two materials, so that even in the case of a defect-free board, only approx. 0.1 % of the initial pressure is transmitted. In the case of a sample with a defect, the transmitted signal even drops to approx. 0.001 %. This amplitude drop is utilized for the detection of delaminations.

To prevent overlapping between the reflected and transmitted waves, a transmitter tilted relative to the plate plane can be used instead of coupling the sound perpendicularly into the plate. Due to the angle, no obvious interference phenomena occur. Burst operation and the angle can ensure permanent, reliable delamination detection that is independent of external influences and movements of the plate.

A major challenge in ultrasonic examination is the measurement up to the edge of the plate. This is because portions of the sound waves impinging on the receiver do not pass through the wood sample, but run laterally next to the panel. These lateral sound waves are hardly attenuated because they are not reflected at the transitions from the sample to the air. Some of these sound waves overlap with the transmitted sound. The result is that a larger sound signal is measured at the receiver and defects can no longer be detected. To ensure complete quality control down to the panel edge despite these edge effects, it is advisable to use acoustic apertures (see Figure 17 a). The aperture prevents the sound from propagating next to the measured material, thus leading to unwanted effects. By arranging the transmitters and apertures to match the width of the plate, it is possible to perform gap detection right up to the edge of the plate. This offers great advantages, especially for narrow board widths, such as applications in the parquet sector. By using several rows with transmitters arranged offset to each other, as shown in Figure 17 b, the areas between the transmitter channels of the first row can also be monitored, thus guaranteeing a full-surface inspection. Thanks to the continuous development in the transmitter and receiver technology as well as the control of the transmitters and data processing, it is possible to measure plates up to a thickness of approx. 65 mm without resonance, depending on the material.

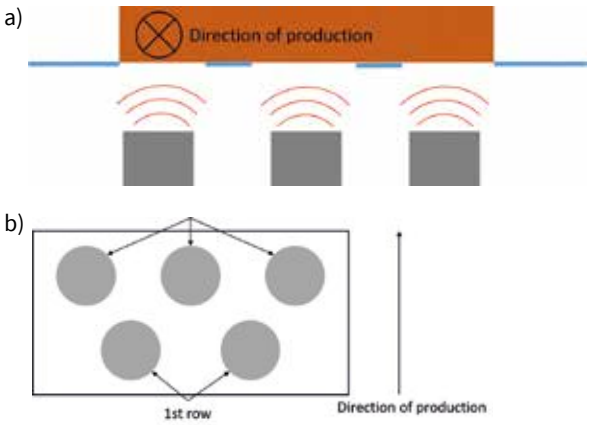

Figure 17: Use of acoustic apertures to eliminate diffraction effects. a) View in production direction. b) Top view of acoustic aperture with two rows.

Wood-delamination detection system are already successful used for quality control of boards up to almost 4 m as well as for inspection of parquet panels (see Figure 18).

Figure 18: Industrial delamination detection on wood-based materials with air-coupled ultrasound. Multiple transmitter/receiver channels are distributed across the width of a panel to ensure complete monitoring during ongoing production.

Automated Air-coupled Ultrasound Testing in Aerospace

(Corresponding Author: Wolfgang Hillger and Artur Szewieczek, Hillger NDT GmbH, Braunschweig, Germany)

In the aerospace sector, standard ultrasonic testing is a common thing. Nevertheless, ACU is not yet as established as it could be in this sector. One example of a successful ACU inspection qualification is the inspection of the Airbus Helicopters H145 helicopter tail boom. An air-coupled ultrasonic system with through-transmission probe arrangement has been applied for a high reliability. It has been combined with a ten axis mechanics. The detection of all relevant defects in the sandwich part of the tail boom has been proved. The system is shown in Figure 20. It is working since the end of 2011 and fulfills all requirements. The size of the system is about 5,3 m x 4,9 m with a height of 10,6 m. A length of 3000 mm and a diameter range from 300 to 1100 mm gives the maximum cylindrical inspection volume. The tail boom is inspected in vertical position. The mechanic consists of two CFRP-beams which are rotatable and adjustable in height each with a three axis pivot arm. The maximum inspection speed is 500 mm/s. The maximum x-offset of the system is ±1 mm. The programming of the track is carried out of a CATIA 3D model of the component.

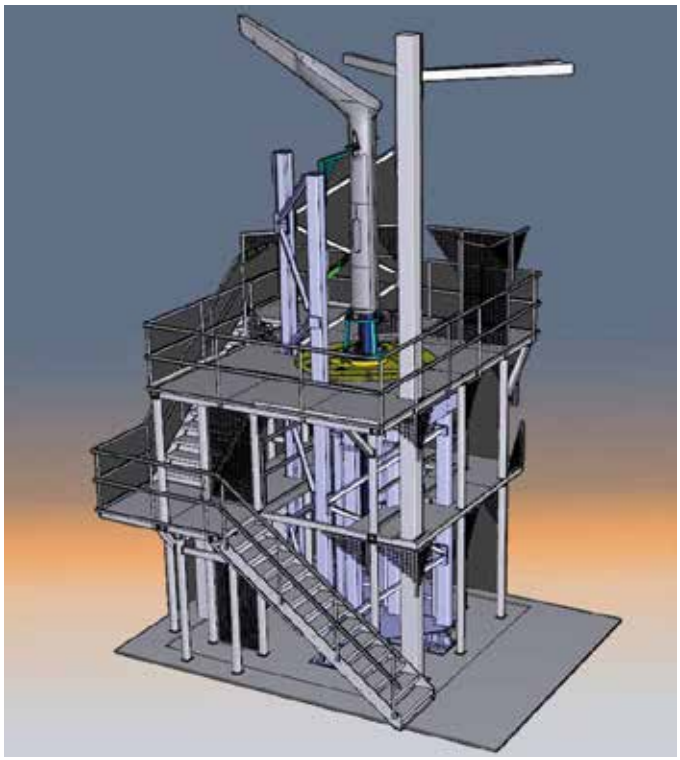

Figure 19: ACU tail boom inspection system (Airbus Helicopters)

One of the largest air-coupled systems in the world is called ANDI and has been installed in Emmen, Switzerland. Two air-coupled transducers in through-transmission investigate the curved component surface. The system is shown in Figure 20. It consists of two robots, one inside the component and one outside. The outer scanning system consists of a FEM-optimized cantilever with a special CFFR robot. It has a half cylinder inspection range with a length of 21.7 m and a width of 5.4 m. The maximum velocity is 1 m/s. The inspection time depends on the scanning grid and takes about 36-72 h. The accuracy reaches less than 2.5 mm, the automatic distance control between the component and the probes provide a tolerance of ±1 mm. (48)

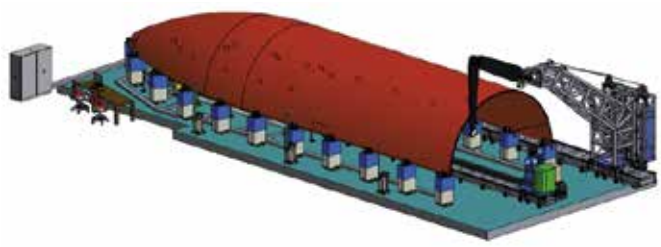

Figure 20: ACU-equipment ANDI for space components with 21 m scanning length

Conclusion

As shown in this article, the non-destructive testing method using air-coupled ultrasound is capable to inspect many kinds of materials. Especially on porous, strongly attenuating or water sensitive materials as well as on all sorts of fiber-reinforced materials, air-coupled ultrasound reveals his advantage of being a contactless and universal testing method. Compared to the well-known ultrasonic testing with coupling agent, air-coupled ultrasonic technique provides constant testing without any coupling liquids and pastes. It prevents all disadvantages of water coupling like corrosion and air-bubbles in the coupling path.

Several research and development projects have been carried out in terms of transducer technology, signal generation/processing, data evaluation and the measuring setup within the last decade. Sales figures increased throughout all areas, and air-coupled ultrasound has become more and more prominent.

However, research and development of the detection system itself is not the last innovative step in air-coupled ultrasonic testing. In times of increasing networking of industrial production systems and optimized process control based on Industry 4.0, obtaining as much product data as possible for quality control in the production process is becoming increasingly important in order to be able to ensure efficient production. An important role in the support of these processes is played by standardization. This was recognized by several German producers of the ultrasonic equipment, scientists and end users, who initiated a network of related experts. Within the frame of the German Society for NDT (DGZfP), they have recently founded the Subcommittee Air-Coupled Ultrasonic Testing (UA ACUT) to discuss regularly the means to promote air-coupled ultrasonic testing, also through adapting existing or creating new national and international standards and norms.

Air-coupled ultrasound is an emerging technique that is being used more and more in industrial practice, having the potential to replace some older non-destructive testing method in the future.

Acknowledgements

The idea for the concept of this review article was born during the discussions of a newly founded Subcommittee Air-coupled Ultrasonic Testing (UA ACUT) of the German Society for Non-Destructive Testing (DGZfP). A vivid exchange of ideas between all members of this group has shaped the thoughts and content of this article. We owe them our gratitude. The authors of individual sections are listed as corresponding authors below the section titles.

References

[1] KUHL, W., G. R. SCHODDER, and F.-K. SCHRÖDER. Condenser transmitters and microphones with solid dielectric for airborne ultrasonics [online]. Acta Acustica united with Acustica. 1954, 4(5), 519-532. Available from: https://www.ingentaconnect.com/content/dav/aaua/1954/00000004/00000005/art00003.

[2] HICKLING, Robert, and Samuel P. MARIN. The use of ultrasonics for gauging and proximity sensing in air [online]. The Journal of the Acoustical Society of America. 1986, 79(4), 1151-1160. Available from: 10.1121/1.393387.

[3] LUUKKALA, M., P. HEIKKILA, and J. SURAKKA. Plate wave resonance — a contactless test method [online]. Ultrasonics. 1971, 9(4), 201-208. Available from: 10.1016/0041-624X(71)90387-8.

[4] FOX, J. D., G. S. KINO, and B. T. KHURI-YAKUB. Acoustic microscopy in air at 2 MHz [online]. Applied Physics Letters. 1985, 47(5), 465-467. Available from: 10.1063/1.96149.

[5] YANO, Tsutomu, Masayuki TONE, and Akira FUKUMOTO. 1 MHz Ultrasonic Transducer Operating in Air. In: A. J. Berkhout, J. Ridder, and L. F. van der Wal, eds. Acoustical Imaging. Boston, MA: Springer US, 1985, pp. 575-584.

[6] SCHILLER, S., C. K. HSIEH, C. CHOU, and B. KHURI-YAKUB. Novel high-frequency air transducers. Review of progress in quantitative NDE. 1990, 795.

[7] SMITH, W. A., and B. A. AULD. Modeling 1-3 composite piezoelectrics: thickness-mode oscillations [online]. IEEE transactions on ultrasonics, ferroelectrics, and frequency control. 1991, 38(1), 40-47. Available from: 10.1109/58.67833.

[8] HUTCHINS, and SCHINDEL. Advances in non-contact and air-coupled transducers [US materials inspection. Proceedings of IEEE Ultrasonics Symposium ULTSYM-94: IEEE, 31 Oct. 1993 - 3 Nov. 1993, 1245-1254 vol.2.

[9] SCHINDEL, D. W., D. A. HUTCHINS, Lichun ZOU, and M. SAYER. The design and characterization of micromachined air-coupled capacitance transducers [online]. IEEE transactions on ultrasonics, ferroelectrics, and frequency control. 1995, 42(1), 42-50. Available from: 10.1109/58.368314.

[10] GEBHARDT, W., P. KREIER, and W. HILLGER. Airborne Ultrasonic Probes: Design, Fabrication, Application. Proceedings / 7th European Conference on Non-Destructive Testing, Copenhagen, 26 - 29 May 1998. Broendy, Denmark, 1998.

[11] BHARDWAJ, M. High transduction piezoelectric transducers and introduction of non-contact analysis. [online]. Available from: https://www.ndt.net/article/v05n01/bhardwaj/bhardwaj.htm.

[12] SCHINDEL, D. W., and D. A. HUTCHINS. Through-thickness characterization of solids by wideband air-coupled ultrasound [online]. Ultrasonics. 1995, 33(1), 11-17. Available from: 10.1016/0041-624X(95)00011-Q.

[13] BLOMME, E., D. BULCAEN, and F. DECLERCQ. Air-coupled ultrasonic NDE: experiments in the frequency range 750kHz–2MHz [online]. NDT & E International. 2002, 35(7), 417-426. Available from: 10.1016/S0963-8695(02)00012-9.

[14] STOESSEL, R., N. KROHN, K. PFLEIDERER, and G. BUSSE. Air-coupled ultrasound inspection of various materials [online]. Ultrasonics. 2002, 40(1-8), 159-163. Available from: 10.1016/s0041-624x(02)00130-0.

[15] DÖRING, Daniel. Luftgekoppelter Ultraschall und geführte Wellen für die Anwendung in der zerstörungsfreien Werkstoffprüfung: Universität Stuttgart, 2011.

[16] GRÄFE, Boris. Luftgekoppeltes Ultraschallecho-Verfahren für Betonbauteile. Zugl.: Berlin, Techn. Univ., Diss., 2008. Berlin: Bundesanstalt für Materialforschung und -prüfung (BAM), 2009. BAM-Dissertationsreihe. 41. 978-3-9812354-4-9.

[17] VÖSSING, Konrad J., Mate GAAL, and Ernst NIEDERLEITHINGER. Imaging wood defects using air coupled ferroelectret ultrasonic transducers in reflection mode [online]. Construction and Building Materials. 2020, 241(6), 118032. Available from: 10.1016/j.conbuildmat.2020.118032.

[18] GAAL, M., J. DÖRING, J. PRAGER, D. BRACKROCK, E. DOHSE, T. HOMANN, and M. GRZESZKOWSKI. Anwendung geführter Ultraschallwellen für die Prüfung von Klebeverbindungen. In: DGZfP, ed. DGZfP-Jahrestagung 2014, 2014.

[19] KIEL, M., R. STEINHAUSEN, and A. BODI. Einseitige Luftultraschallprüfung von Blech-verbindungen - Eine Sache der Geometrie. In: DGZfP, ed. Berichtsband DGZfP Jahrestagung 2017, 2017.

[20] WEVERS, M., and M. SURGEON. Acoustic Emission and Composites. Comprehensive Composite Materials: Elsevier, 2000, pp. 345-357.

[21] MCLASKEY, Gregory C., Steven D. GLASER, and Christian U. GROSSE. Beamforming array techniques for acoustic emission monitoring of large concrete structures [online]. Journal of Sound and Vibration. 2010, 329(12), 2384-2394. Available from: 10.1016/j.jsv.2009.08.037.

[22] MOVAHED, Ali, Thomas WASCHKIES, and Ute RABE. Air Ultrasonic Signal Localization with a Beamforming Microphone Array [online]. Advances in Acoustics and Vibration. 2019, 2019, 1-12. Available from: 10.1155/2019/7691645.

[23] VERFAHREN UND ANORDNUNG ZUR ORTSAUFGELÖSTEN ERFASSUNG VON SCHALLEMISSIONEN, INSBESONDERE ULTRASCHALLEMISSIONEN - European Patent Office - EP 3748397 A1. Inventor: Thomas WASCHKIES, Ute RABE, Florian RÖMER, and Giovanni DEL GALDO. EP3748397A1.

[24] MATSUO, T., and D. HATANAKA. Air ultrasonic signal localization with a beamforming microphone array. Advances in Acoustics and Vibration. 2019, (12).

[25] CAE SOFTWARE AND SYSTEMS (N.D.). Acoustic Camera/Sound Source Localization- Noise Inspector. [online]. 12 November 2020, 12:00. Available from: https://www.cae-systems.de.

[26] PFEIFFER, H., M. BÖCK, I. PITROPAKIS, A. SZEWIECZEK, W. HILLGER, and C. GLORIEUX. Identification of impact damage in sandwich composites by acoustic camera detection of leaky Lamb wave mode conversions. e-Journal of Non-Destructive Testing. 2013, 1435-4934.

[27] FISCHER, Balthasar. Optical microphone hears ultrasound [online]. Nature Photonics. 2016, 10(6), 356-358. Available from: 10.1038/nphoton.2016.95.

[28] FISCHER, Balthasar, Fabrizio SARASINI, Jacopo TIRILLÒ, Fabienne TOUCHARD, Laurence CHOCINSKI-ARNAULT, David MELLIER, Nils PANZER, Ryan SOMMERHUBER, Pietro RUSSO, Ilaria PAPA, Valentina LOPRESTO, and Romain ECAULT. Impact damage assessment in biocomposites by micro-CT and innovative air-coupled detection of laser-generated ultrasound [online]. Composite Structures. 2019, 210, 922-931. Available from: 10.1016/j.compstruct.2018.12.013.

[29] BRAUNS, Matthias, Fabian LUCKING, Balthasar FISCHER, Clint THOMSON, and Igor IVAKHNENKO. Laser-Excited Acoustics for Contact-Free Inspection of Aerospace Composites [online]. Materials Evaluation. 2021, 79(1), 28-37. Available from: 10.32548/2020.me-04188

[30] SESSLER, G. M., and J. HILLENBRAND. Electromechanical response of cellular electret films [online]. Applied Physics Letters. 1999, 75(21), 3405-3407. Available from: 10.1063/1.125308.

[31] PAAJANEN, Mika, Jukka LEKKALA, and Kari KIRJAVAINEN.

ElectroMechanical Film (EMFi) — a new multipurpose electret material [online]. Sensors and Actuators A: Physical. 2000, 84(1-2), 95-102. Available from: 10.1016/S0924-4247(99)00269-1.

[32] BAUER, Siegfried, Reimund GERHARD-MULTHAUPT, and Gerhard M. SESSLER. Ferroelectrets: Soft Electroactive Foams for Transducers [online]. Physics Today. 2004, 57(2), 37-43. Available from: 10.1063/1.1688068.

[33] GAAL, Mate, Rui CALDEIRA, Jürgen BARTUSCH, and Mario KUPNIK. Air-Coupled Ultrasonic Ferroelectret Receiver with Additional DC Voltage [online]. Proceedings. 2017, 1(4), 362. Available from: 10.3390/proceedings1040362.

[34] EALO, Joao L., Jose Carlos PRIETO, and Fernando SECO. Dynamic response estimation of multilayer ferroelectret-based transducers using lumped-element electromechanical models. 2009 IEEE International Ultrasonics Symposium: IEEE, 20 Sep. 2009 - 23 Sep. 2009, pp. 2754-2757.

[35] GAAL, Mate, Jürgen BARTUSCH, Elmar DOHSE, Florian SCHADOW, and Enrico KÖPPE. Focusing of ferroelectret air-coupled ultrasound transducers: AIP Publishing LLC, 2016, p. 80001.

[36] STREICHER, Alexander. Luftultraschall-Sender-Empfänger-System für einen künstlichen Fledermauskopf. Erlangen, Nürnberg, Univ., Diss., 2008.

[37] WEGENER, Michael, Steffen BERGWEILER, Werner WIRGES, Andreas PUCHER, Enis TUNCER, and Reimund GERHARD-MULTHAUPT. Piezoelectric two-layer stacks of cellular polypropylene ferroelectrets: transducer response at audio and ultrasound frequencies [online]. IEEE transactions on ultrasonics, ferroelectrics, and frequency control. 2005, 52(9), 1601-1607. Available from: 10.1109/TUFFC.2005.1516033.

[38] PAZOS-OSPINA, J. F., J. L. EALO, and J. CAMACHO. New dual-focalization ferroelectret-based array for air-coupled ultrasonic inspection of textiles [online]. NDT & E International. 2015, 74, 50-57. Available from: 10.1016/j.ndteint.2015.04.007.

[39] GAAL, Mate, Daniel KOTSCHATE. New technologies for air-coupled ultrasonic transducers.

[40] FELDMAN, K. T. Review of the literature on Rijke thermoacoustic phenomena [online]. Journal of Sound and Vibration. 1968, 7(1), 83-89. Available from: 10.1016/0022-460X(68)90159-4.

[41] DASCHEWSKI, Maxim, Marc KREUTZBRUCK, Jens PRAGER, Elmar DOHSE, Mate GAAL, and Andrea HARRER. Resonanzfreie Messung und Anregung von Ultraschall [online]. tm - Technisches Messen. 2015, 82(3). Available from: 10.1515/teme-2014-0020.

[42] BUCKLEY, J., and R. SERVENT. Improvements in ultrasonic inspection of resistance spot welds [online]. Insight - Non-Destructive Testing and Condition Monitoring. 2009, 51(2), 73-77. Available from: 10.1784/INSI.2009.51.2.73.

[43] ACEBES, Montserrat, Rafael Delgado DE MOLINA, Iñaki GAUNA, Nigel THORPE, and Juan Carlos GUERRO. Development of an automated ultrasonic inspection device for quality control of spot welds. In: Deutscher Gesellschaft für Zerstöungsfreie Prüfung, ed. Proceedings WCNDT 2016.

[44] ROHRINGER, Wolfgang, Thomas HEINE, Ryan SOMMERHUBER, Nico LEHMANN, and Balthasar FISCHER. Optical Microphone as Laser-Ultrasound Detector. Deutsche Jahrestagung für Akustik, 2018.

[45] LEHMANN, Nico, and Sven JUETTNER. Contribution to the Qualification of Air-coupled Ultrasound as Non-destructive, Automated Test Method for Spot Welds in the Car Body Shop. 15th Asia Pacific Conference for Non-Destructive Testing, 2017.

[46] GOMEZ ALVAREZ-ARENAS, T. E. Air-coupled Ultrasonic Transducers. In: Mar Villamiel, Antonia Montilla, José V. García-Pérez, Juan A. Cárcel, and Jose Benedito, eds. Ultrasound in Food Processing. Chichester, UK: John Wiley & Sons, Ltd, 2017, pp. 175-228.

[47] FANG, Yiming, Lujun LIN, Hailin FENG, Zhixiong LU, and Grant W. EMMS. Review of the use of air-coupled ultrasonic technologies for nondestructive testing of wood and wood products [online]. Computers and Electronics in Agriculture. 2017, 137, 79-87. Available from: 10.1016/j.compag.2017.03.015.

[48] SZEWIECZEK, Artur, W. HILLGER, Lutz BÜHLING, and Detlef ILSE. New Developments and applications for Air Coupled Ultrasonic Imaging Systems, 2018.